







## Original Research Article

# Surfactant-Assisted Co-Precipitation Synthesis of Ca-Doped Ceria Nanoparticles for Antibacterial Applications

Ibrahim A. Amar<sup>1,2\*</sup> , Shamsi A. Shamsi<sup>3</sup> , Ruqayah M. Saheem<sup>1</sup>, Amdallah A. Altawati<sup>1</sup>, Mohammed A. Abdulkarim<sup>1</sup>, Mabroukah A. Abdulqadir<sup>1</sup> , Ihssin A. Abdalsamed<sup>1</sup> 

<sup>1</sup> Department of Chemistry, Faculty of Science, Sebha University, Sebha, Libya

<sup>2</sup> Central Laboratory at Sebha University, Sebha, Libya

<sup>3</sup> Department of Botany (Microbiology Lab), Faculty of Science, Sebha University, Sebha, Libya

## ARTICLE INFO

## Article history

Submitted: 08 September 2020

Revised: 28 September 2020

Accepted: 13 October 2020

Available online: 14 October 2020

Manuscript ID: [AJCA-2009-1210](#)

DOI: [10.22034/AJCA.2020.247227.1210](#)

## KEYWORDS

Cerium oxide nanoparticles

Surfactant

Co-precipitation method

Antibacterial activity

Drug-resistance bacteria

Optical density measurement

## ABSTRACT

Antibiotic-resistant pathogenic bacteria (*e.g.*, multi-drug resistant bacteria, MDR) have been one of the major threats to human health. Nanoparticles, the newly emerging tools, hold the promise to solve the antibiotic resistance-related problems. This study aimed at evaluating the antibacterial activities of Ca-doped ceria nanoparticles (CDC) against the Gram-negative bacteria (*Pseudomonas aeruginosa* and *Klebsiella pneumoniae*) and Gram-positive bacteria (*Staphylococcus aureus*) using optical density measurement. Co-precipitation method was used to synthesize the Ca-doped ceria nanoparticles with and without addition of cetyltrimethylammonium bromide (CTAB, cationic surfactant). The prepared nanoparticles were characterized using the X-ray diffraction (XRD), Fourier transform infrared spectroscopy (FTIR), and UV-Vis spectroscopy. The XRD results demonstrated that, the CDC-CTAB nanoparticles (synthesized *via* CTAB-assisted co-precipitation method) had the smaller crystallite size (16.26 nm) and higher specific surface area (56.72 m<sup>2</sup>/g) compared to the CTAB-free synthesized sample (CDC nanoparticles). In addition, the CDC-CTAB nanoparticles exhibited a better inhibition percentage of bacteria growth (29.54-34.08%) against both the Gram-negative and Gram-positive bacteria. In terms of materials cost and toxicity, Ca-doped ceria nanoparticles can be considered as promising materials and, their biological activity might be evaluated against other microorganisms.

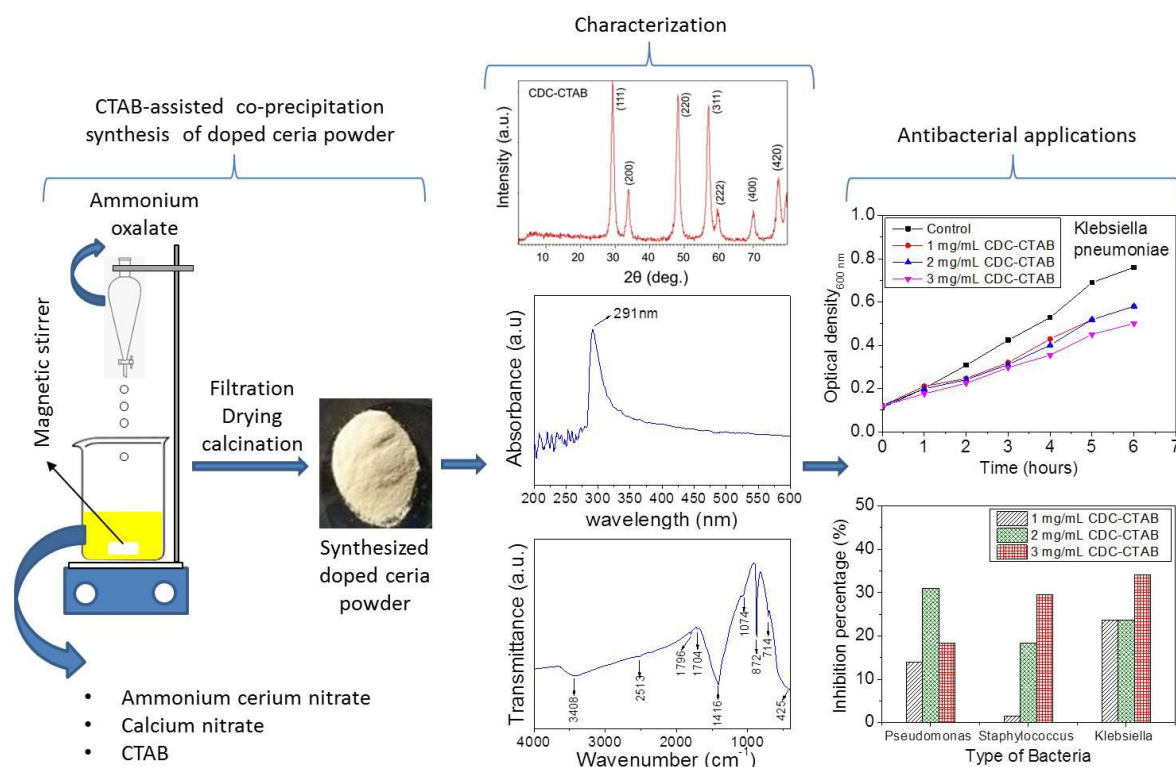
\* Corresponding author: Amar, Ibrahim A.

✉ E-mail: [ibr.amar@sebhau.edu.ly](mailto:ibr.amar@sebhau.edu.ly)

☎ Tel number: +002189451730680000

© 2020 by SPC (Sami Publishing Company)

## GRAPHICAL ABSTRACT



## Introduction

The emergence of drug-resistant pathogenic bacteria is one of the main threats to human health, globally [1-3]. Among these, multi-drug resistant bacteria, MDR, (e.g., *Pseudomonas aeruginosa*, *Klebsiella pneumoniae* and *Staphylococcus aureus*) are considered as one of the most causes of hospital infections [4-7]. According to the World Health Organization (WHO), drug-resistant diseases already led to worldwide annual deaths of at least 700,000, and if no action is taken the figure is projected to increase up to 10 million deaths by 2050 [8]. Nanoparticles (NPs), the newly emerging tools, hold the promise not only to combat antibiotic-resistant bacteria but also serve as antibiotics carrier due to their tailorable physical and chemical properties [2, 9]. Several nanoparticle-based materials including, silver (AgNPs), gold (AuNPs), copper (CuNPs), magnesium oxide (MgO NPs), copper oxide (CuO NPs) zinc oxide (ZnO NPs), titanium oxide (TiO<sub>2</sub> NPs), iron oxide

(Fe<sub>3</sub>O<sub>4</sub> NPs) and cerium oxide (CeO<sub>2</sub> NPs) [2, 9-12] exhibited outstanding antibacterial activities. However, many of these nanomaterials such as AgNPs and CuNPs are highly toxic, even at low doses, to normal human cells [10, 13, 14].

In recent years, cerium oxide nanoparticles (CeO<sub>2</sub> NPs) or nanoceria based-nanoparticles have attracted considerable interest due to their properties such as; unique antibacterial mechanism, redox behavior of cerium (Ce<sup>3+</sup>/Ce<sup>4+</sup>), and low or even no toxicity to mammalian cells [9, 10, 15]. Thus, CeO<sub>2</sub> NPs have found widespread biomedical applications such as, anti-inflammation [16], antibacterial activities [17], immunosensors [18], antioxidant [19], anticancer [20], and drug delivery device [21]. In regards to the antibacterial applications, several undoped CeO<sub>2</sub> NPs [17, 22] and doped-CeO<sub>2</sub> NPs such as; Sm-doped CeO<sub>2</sub> [23], Co-doped CeO<sub>2</sub> [24], Cu-doped CeO<sub>2</sub> [20] and Gd-doped CeO<sub>2</sub> [25] and Ag-doped CeO<sub>2</sub> [17] are being tested as antibacterial agents against Gram-positive (e.g.,

*Staphylococcus aureus*, *Bacillus cereus*) and Gram-negative (e.g., *Escherichia coli*, *Klebsiella pneumoniae*, *Pseudomonas aeruginosa*) bacteria.

In recent years, doped ceria nanoparticles containing calcium (Ca) have gained much attention, as Ca is readily available and low in cost compared to other dopants (Sm and Gd) [26, 27]. Ca-doped ceria NPs have been utilized in many applications such as; solid oxide fuel cells (SOFCs) [28], dye photocatalytic degradation [29], and ultraviolet filtration [30]. Cerium oxide-based nanoparticles are synthesized using different methods including, solid-state reaction, sol-gel, co-precipitation, hydrothermal, solvothermal, microemulsion, ball milling, and combustion [12, 15, 31]. Among these, co-precipitation is a simple, low in cost and industrially viable method [22, 32]. Besides, surfactants including; sodium dodecyl sulfate (SDS, anionic) and cetyltrimethylammonium bromide (CTAB, cationic) are added during the synthesis of nanomaterials to obtain less agglomerated nanoparticle with high surface area and enhanced catalytic activity [33-35]. To the best of author's knowledge, there are no reports on CTAB-assisted co-precipitation synthesis of Ca-doped  $\text{CeO}_2$  NPs and their antibacterial activity. Therefore, this work aims to synthesize Ca-doped  $\text{CeO}_2$  NPs using CTAB-assisted co-precipitation method and evaluate their antibacterial activity against *Pseudomonas aeruginosa*, *Klebsiella pneumoniae* and *Staphylococcus aureus* by the optical density measurement method.

## Experimental

### Materials

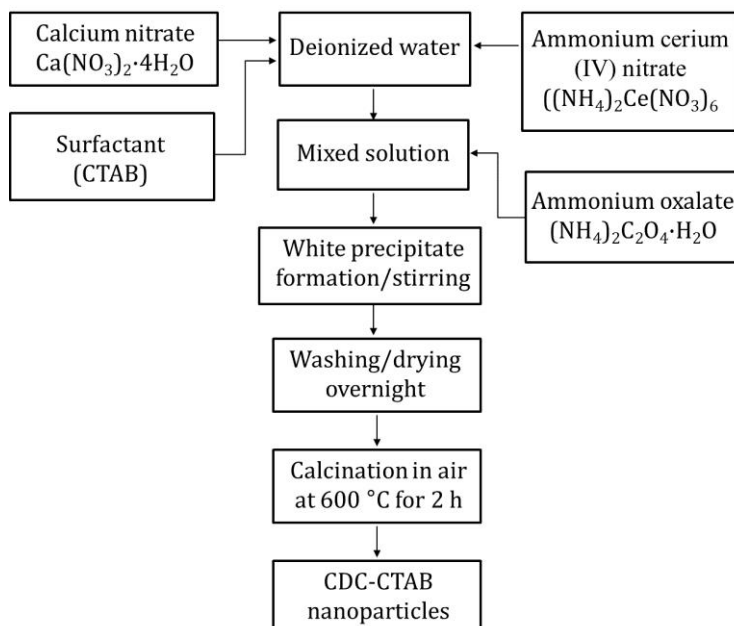
Ammonium oxalate  $((\text{NH}_4)_2\text{C}_2\text{O}_4 \cdot \text{H}_2\text{O})$  and calcium nitrate  $(\text{Ca}(\text{NO}_3)_2 \cdot 4\text{H}_2\text{O})$  were purchased from T-Barker Lab Chemicals, Ammonium cerium (IV) nitrate  $((\text{NH}_4)_2\text{Ce}(\text{NO}_3)_6)$  was obtained from the VWR Prolabo BDH Chemicals.

Cetyltrimethylammonium bromide, CTAB,  $(\text{CH}_3(\text{CH}_2)_{15}(\text{CH}_3)_3\text{NBr})$  was purchased from Park scientific Ltd. Dimethyl sulphoxide, DMSO,  $((\text{CH}_3)_2\text{SO})$  purchased from Carlo Ebra. Casein and yeast extract were obtained from Sigma. Sodium chloride (NaCl) was purchased from Scharlau. The isolated bacteria (*Pseudomonas aeruginosa*, *Staphylococcus aureus* and *Klebsiella pneumoniae*) were kindly provided by Department of Botany (Microbiology Lab), Faculty of Science, Sebha University, Sebha, Libya.

### Ca-Doped ceria nanoparticles synthesis

Surfactant-assisted co-precipitation method was employed to synthesize Ca-doped ceria ( $\text{Ce}_{0.8}\text{Ca}_{0.2}\text{O}_{2-\delta}$ , CDC-CTAB) using CTAB as a cationic surfactant and ammonium oxalate as a precipitating agent. In a typical experiment, stoichiometric amounts of  $(\text{NH}_4)_2\text{Ce}(\text{NO}_3)_6$  and  $\text{Ca}(\text{NO}_3)_2 \cdot 4\text{H}_2\text{O}$  were dissolved in deionized water ( $\sim 50$  mL). Then, CTAB (0.3 mol) was added to the mixed nitrate solution under continues stirring [36]. CTAB (capping agent) will reduce the surface tension of the precursor solution [37]. Afterwards, the ammonium oxalate solution (0.3 M) was added dropwise at room temperature, under the vigorous stirring to the mixed solution. The resulting white precipitate stirred for 1 h for hominization, vacuum filtrated and washed several times with deionized water before being overnight dried. Finally, the dried solid material was calcined in air at  $600^\circ\text{C}$  for 2 h to get CDC-CTAB nanopowder (pale-yellow). Figure 1 shows a diagram of CTAB-assisted co-precipitation synthesis of ca-doped ceria (CDC-CTAB). Ca-doped ceria ( $\text{Ce}_{0.8}\text{Ca}_{0.2}\text{O}_{2-\delta}$ , CDC) also synthesized *via* a co-precipitation process but without CTAB surfactant addition (surfactant-free synthesis), as described elsewhere [29, 38].

**Figure 1.** A schematic representation of CTAB-assisted co-precipitation synthesis of Ca-doped ceria ( $\text{Ce}_{0.8}\text{Ca}_{0.2}\text{O}_{2-\delta}$ , CDC-CTAB)



### Characterization

The phase purity of the prepared samples (CDC and CDC-CTAB) was evaluated using Philips – PW 1800 X-ray diffractometer (XRD) using  $\text{CuK}\alpha$  radiation ( $\lambda=1.54186 \text{ \AA}$ ). The structural parameters were estimated using the following Equations 1-5.

$$a = d_{hkl} \sqrt{h^2 + k^2 + l^2} \quad (1)$$

$$D = \frac{0.9 \lambda}{(\beta \cos \theta)} \quad (2)$$

$$V_{\text{cell}} = a^3 \quad (3)$$

$$\rho_{\text{XRD}} = \frac{ZM}{N_A V_{\text{cell}}} \quad (4)$$

$$S_{\text{XRD}} = \frac{6000}{D \cdot \rho_{\text{XRD}}} \quad (5)$$

where,  $a$  is the lattice constant,  $hkl$  are the Miller indices and  $d$  is the interplanar distance.  $D$  is the average crystallite size (nm),  $\lambda$  is the wavelength of the X-ray,  $\theta$  is the Bragg angle and  $\beta$  is the full width at half maximum, FWHM, (in radian) of the peak.  $\rho_{\text{XRD}}$  is the X-ray density,  $Z$  is the number of molecules per formula unit ( $Z = 4$  for fluorite system),  $N_A$  is the Avogadro's number,  $V_{\text{cell}}$  is the unit cell volume,  $M$  is the sample molecular weight (g/mol) and  $S_{\text{XRD}}$  is the specific surface area ( $\text{m}^2/\text{g}$ ).

Nicolet 380 spectrometer was used to record the Fourier transform infrared spectra (FTIR) of the prepared CDC and CDC-CTAB samples in KBr pellets within the wavenumber ranging from 400 to  $4000 \text{ cm}^{-1}$ . The UV-Vis analysis of CDC and CDC-CTAB samples was carried out using Evolution 300 spectrophotometer (Thermo Electronic Corporation). First, 1 mg of doped ceria samples were transferred to a small glass bottle containing 25 mL of ethanol before being ultra-sonicated for 30 min and then their UV-Vis spectra were recorded within the wavelength of 200 to 600 nm using quartz cuvettes (1 cm in length) [30]. The band-gap energy ( $E_g$  (eV) =  $1240/\lambda$ ) values of both sample (CDC and CDC-CTAB) can be estimated using the following Tauc's relation ( $(ah\nu)^2$  against  $h\nu$  plot) [39, 40].

$$(ah\nu)^n = B(h\nu - E_g) \quad (6)$$

Where,  $\lambda$  is the wavelength corresponding to the sample absorption peak,  $B$  is a constant,  $\alpha$  is the absorption coefficient and  $h\nu$  is the photon energy (eV). The  $n$  value equals 2 and  $\frac{1}{2}$  for direct and indirect transitions, respectively.

### Antibacterial activity test

Antibacterial potential of CDC and CDC-CTAB nanoparticles were evaluated against *Pseudomonas aeruginosa*, *Klebsiella pneumoniae* and *Staphylococcus aureus* by the optical density measurement method. In this study, LB broth medium (containing 10 g/L casein, 5 g/L yeast extract and 5 g/L NaCl, sterilized in an autoclave (Astell) at 120-121 °C for 15 min) was used to culture the bacteria strains. In brief, 5 mL of LB broth medium was transferred into clean and sterilized test tubes to which 1 µL of bacteria suspension was added. Then, the test tubes were closed with sterilized cotton, shaken at 140 rpm using a vortex (Stuart) and incubated for 24 h before use. The solution of both synthesized nanoparticles (CDC and CDC-CTAB) at a concentration of 1, 2 and 3 mg/mL were

prepared using 5% DMSO solution. The bacteria growth was monitored in the absence and the presence of nanoparticles. 1 mL of the prepared nanoparticle solutions (1 to 3 mg/mL) was added to test tubes containing sub-cultured strains (5 mL of LB broth and 1 µL of bacteria suspension) and vortexed. Samples containing only bacteria strains and culture medium (without nanoparticles) were used as control samples. Then, the samples were incubated for 6 h at 37 °C. The optical density at 600 nm ( $OD_{600}$ ) of the samples was measured at a different time of incubation 0, 1, 2, 3, 4, 5, 6 h using UV-Vis spectrophotometer (Jenway model 6305, UK). The inhibition percentage of bacteria growth was estimated from  $OD_{600}$  after 6 hours of incubation using the Equation 7.

$$\text{Inhibition percentage (\%)} = \frac{OD_{\text{control sample}} - OD_{\text{treated sample}}}{OD_{\text{control sample}}} \times 100 \quad (7)$$

Where,  $OD_{\text{control sample}}$  and  $OD_{\text{treated sample}}$  are the optical density in absence and presence of the synthesized nanoparticles, respectively.

For the statistical analysis, each optical density measurement was triplicated and the resulted was reported as the mean  $\pm$  standard deviation. Statistical package for the social sciences (SPSS) software (version 17) was used for this purpose. One-way analysis of variance (ANOVA) was performed and  $P$  value  $< 0.05$  probability level was considered statistically significant.

## Results and Discussion

### Characterization

Figures 2a and b show the XRD patterns of non-surfactant (CDC) and surfactant-assisted co-precipitation synthesis (CDC-CTAB) of calcium-doped cerium oxide nanoparticles ( $\text{Ce}_{0.8}\text{Ca}_{0.2}\text{O}_{2-\delta}$ ), respectively. As shown, the calcination of CDC (Figure 2a) and CDC-CTAB (Figure 2b) precursors in the air at 600 °C for 2 h resulted in

the formation of a single-phase. Besides, in both cases, the diffraction peaks were well indexed to the cubic fluorite structure of cerium oxide,  $\text{CeO}_2$ , (JCPDS card No. 34-0394). The most intense peaks were used to estimate the crystal structure parameters including; lattice constant ( $a=b=c$ ), unit cell volume ( $V_{\text{cell}}$ ), the crystallite size ( $D$ ), the X-ray density ( $\rho_{\text{XRD}}$ ) and the specific surface area ( $S_{\text{XRD}}$ ). In the case of CDC, the values were estimated to be 5.3821 Å, 154.54 Å<sup>3</sup>, 23.93 nm, 6.54 g/cm<sup>3</sup> and 24.54 m<sup>2</sup>/g for  $a$ ,  $V_{\text{cell}}$ ,  $D$ ,  $\rho_{\text{XRD}}$  and  $S_{\text{XRD}}$ , respectively. For CDC-CTAB, the values were approximately 5.3742 Å, 155.22 Å<sup>3</sup>, 16.26 nm, 6.51 g/cm<sup>3</sup> and 56.72 m<sup>2</sup>/g for  $a$ ,  $V_{\text{cell}}$ ,  $D$ ,  $\rho_{\text{XRD}}$  and  $S_{\text{XRD}}$ , respectively. The XRD data revealed that the sample synthesized using CTAB as a surfactant (CDC-CTAB) exhibited the smaller average crystallite size ( $D$ ) and higher surface area ( $S_{\text{XRD}}$ ) compared to a non-surfactant synthesized sample (CDC), as mentioned above.

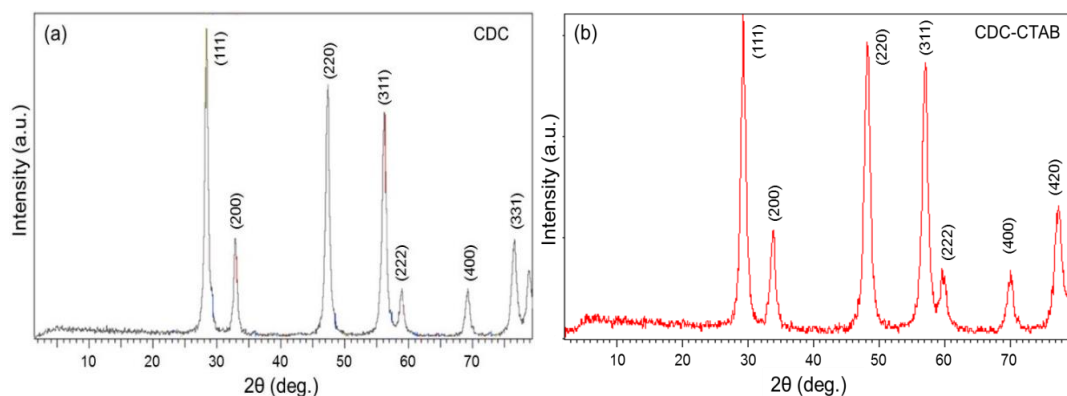


**Figure 2.** Powder X-ray diffraction patterns. (a) CDC powder; (b) CDC-CTAB powder

Figures 3a and b display the FTIR spectra in the wavenumber range of 400 to 4000  $\text{cm}^{-1}$  of CDC and CDC-CTAB powders, respectively. As shown, both samples (CDC and CDC-CTAB) exhibited almost similar FTIR spectra. In both cases, the bands located within the range of 425 and 568  $\text{cm}^{-1}$  are due to the vibration of Ce-O bond [41]. The absorption bands located approximately in the wavenumber ranging from 713 to 1074  $\text{cm}^{-1}$  are ascribed to the stretching vibration of C-O bond [42]. The bands at 1419 (Figure 3a) and 1416  $\text{cm}^{-1}$  (Figure 3b) are ascribed to the

bending vibration of C-H bond [43]. The weak bands located at 1705 (Figure 3a) and 1704  $\text{cm}^{-1}$  (Figure 3b) are due to C=O group [20]. The weak absorption bands appears within the wavenumber range of 2518 and 2513  $\text{cm}^{-1}$  are ascribed to atmospheric or dissolved  $\text{CO}_2$  [24]. The weak bands located at 1797 (Figure 3a) and 1769  $\text{cm}^{-1}$  (Figure 3b) the bending vibration of O-H bond [44]. The broad bands located at 3429 and 3408 are due to the stretching vibration of O-H bond for CDC and CDC-CTAB samples, respectively [25, 44]

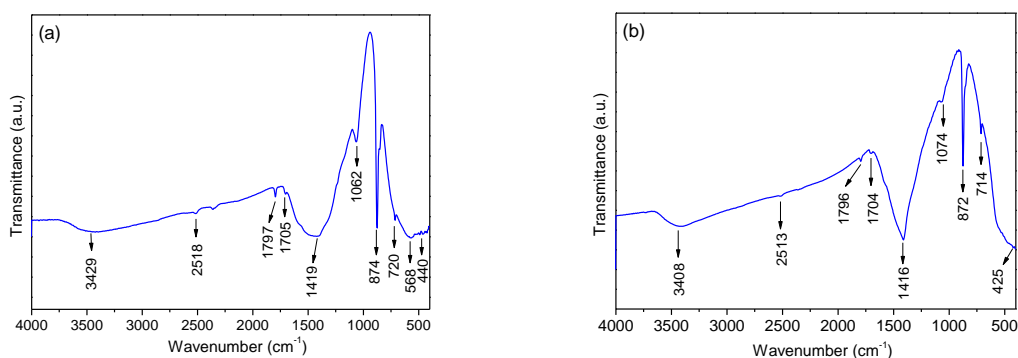


**Figure 3.** FTIR spectra. (a) CDC nanoparticles; (b) CDC-CTAB nanoparticles

In this study, UV-Vis spectroscopy was employed to investigate the optical properties of CDC and CDC-CTAB nanoparticles. The UV-Vis absorption spectra within the wavelength ranging from 200 to 600 nm for CDC and CDC-CTAB samples dispersed in ethanol are

presented in Figures 4a and b, respectively. As shown, the maximum absorption peaks located approximately at 292 and 291 nm for CDC and CDC-CTAB samples, respectively. These values are similar that reported for cerium oxide (292 nm) and indicating  $\text{CeO}_2$  nanoparticles formation



[45]. Besides, the band-gap energies ( $E_g$ ) for CDC and CDC-CTAB samples were estimated from Tauc plots, as shown in Figure 5. The  $E_g$  value of CDC was 3.64 eV (Figure 5a), whereas that of CDC-CTAB was about 3.91 eV (Figure 5b). The

obtained  $E_g$  values of CDC and CDC-CTAB are higher than that reported for undoped  $\text{CeO}_2$  (3.20 eV) [30] and lower than that of Ca-doped  $\text{CeO}_2$  (3.96 eV) [29].

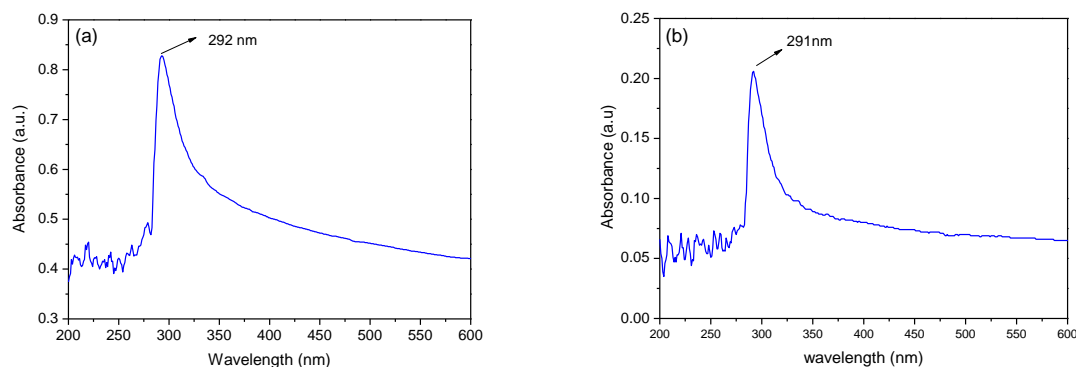


**Figure 4.** UV-Vis absorption spectra. (a) CDC nanoparticles; (b) CDC-CTAB nanoparticles

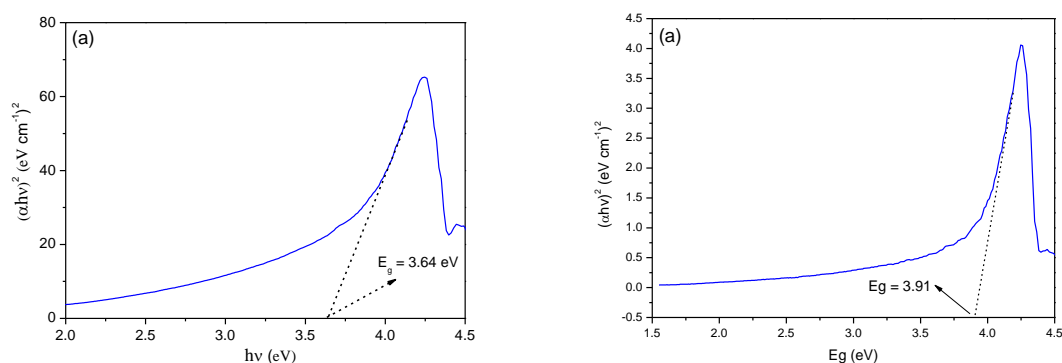


**Figure 5.** Tauc plots. (a) CDC nanoparticles; (b) CDC-CTAB nanoparticles

#### Antibacterial activity of synthesized nanoparticles

The antibacterial activities of CDC (surfactant-free synthesized) and CDC-CTAB (surfactant-assisted synthesized) nanoparticles were evaluated against the Gram-negative bacteria (*Pseudomonas aeruginosa* and *Klebsiella pneumoniae*) and Gram-positive bacteria (*Staphylococcus aureus*) by the optical density measurement method. The optical densities were measured at 600 nm ( $OD_{600}$ ) in LB broth medium at 0, 1, 2, 3, 4, 5 and 6 h in the absence (control) and presence of the synthesized Ca-doped ceria

nanoparticles. Figure 6 shows the bacterial growth of *Pseudomonas aeruginosa* (Figure 6a), *Klebsiella pneumoniae* (Figure 6b) and *Staphylococcus aureus* (Figure 6c) in the absence (control sample) and the presence of different amounts of CDC nanoparticles (1-3 mg/mL) as a function of incubation time. As shown, the optical density increases with time in all cases, indicating the growth of bacteria. However, the optical density values in the presence of CDC nanoparticles were low compared with those obtained for the control sample (*i.e.*, bacteria in culture medium), indicating the decrease in

bacterial growth. Besides, after 6 hours of incubation, the optical density values for *Pseudomonas aeruginosa* (Gram-negative) and *Staphylococcus aureus* (Gram-positive) bacteria decreased with increasing the amount of CDC nanoparticles from 1 to 3 mg/mL, indicating the decreased bacterial growth, as shown in Figures 6a and c respectively. This can be ascribed to in the increase in the surface area of CDC nanoparticles that is in contact with the membrane of bacterial cells. This nanoparticles-membrane contact may influence the cellular response by increasing the permeability of the outer cell membrane which leads to CDC nanoparticles entry into the cells [46]. In the case of *Klebsiella pneumoniae* bacteria (Gram-negative), after 6 hours of incubation, the optical density increased with increasing CDC nanoparticles amount from 1 to 2 mg/mL after which it was decreased as the CDC nanoparticles increased to 3 mg/mL, as shown in Figure 6b. This might be due to aggregation of CDC nanoparticles with increasing their amounts which in turn resulted in reducing their area of

contact with the bacterial cell membrane. Figure 7 depicts the growth curve of *Pseudomonas aeruginosa* (Figure 7a) and *Klebsiella pneumoniae* (Figure 7b) and *Staphylococcus aureus* (Figure 7c) bacteria treated with different amount of CDC-CTAB nanoparticles (1 to 3 mg/mL) as a function of incubation time (0 to 6 hours). As observed in the case of CDC nanoparticles, the optical density values increase with time in all cases (control sample and in the presence of CDC-CTAB nanoparticles, which indicates the bacterial growth, as shown in Figure 7. However, the increase of the optical density with the incubation time (0 to 6 h) in the presence of CDC-CTAB nanoparticles was less compared to that observed in the control sample, which indicates the decreased bacterial growth as mentioned above. Also, the optical density values decreased with increasing CDC-CTAB amounts from 1 to 3 mg/mL in all cases, which might be due to in the increase of the area of contact between the membrane of bacterial cells and CDC-CTAB nanoparticles as mentioned previously.

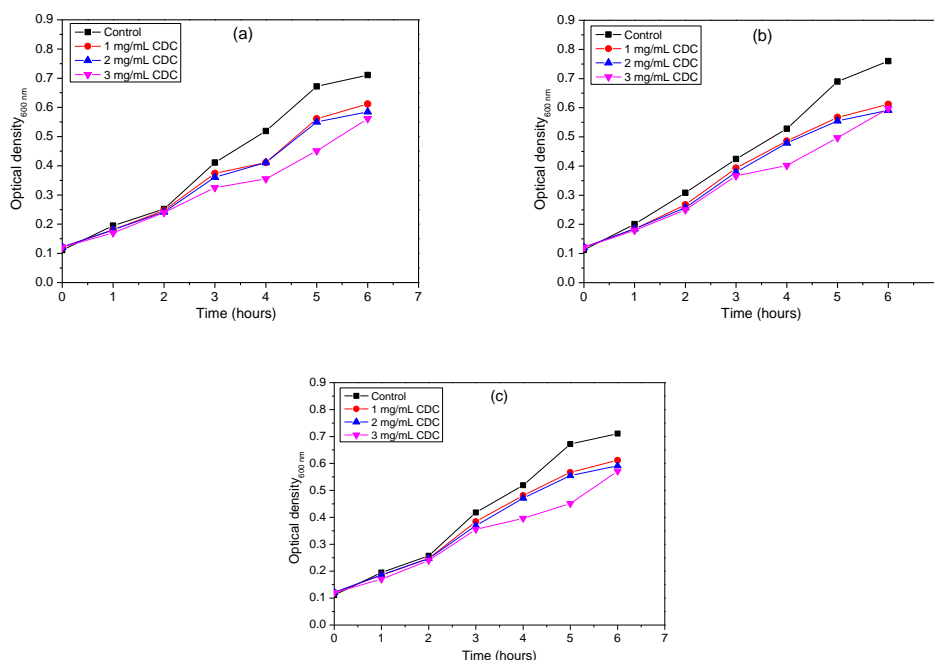


**Figure 6.** Growth curves of various bacteria treated with different amounts of CDC nanoparticles. (a) *Pseudomonas aeruginosa*; (b) *Klebsiella pneumoniae*; (c) *Staphylococcus aureus*. ( $P < 0.05$ )



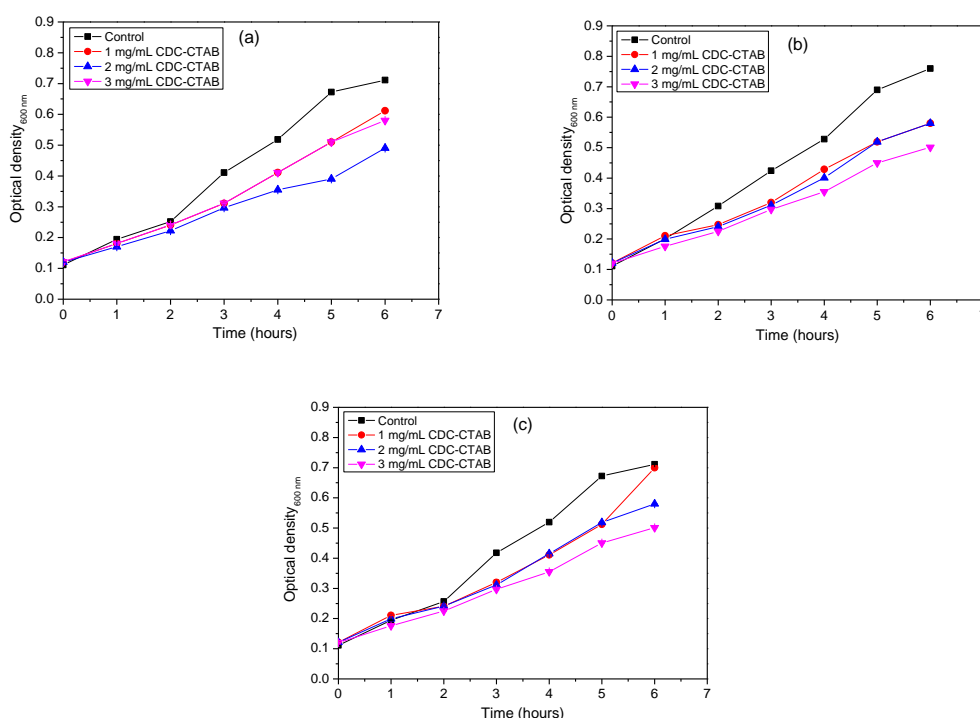


**Figure 7.** Growth curves of various bacteria treated with different amounts of CDC-CTAB nanoparticles. (a) *Pseudomonas aeruginosa*; (b) *Klebsiella pneumoniae*; (c) *Staphylococcus aureus*. ( $P < 0.05$ )

Figure 8 shows the inhibition percentage (%), after 6 h of incubation, of *Pseudomonas aeruginosa*, *Klebsiella pneumoniae* and *Staphylococcus aureus* bacteria treated with different amounts of Ca-doped ceria nanoparticles (1 to 3 mg/mL). In general, the CDC-CTAB sample, which synthesized using the CTAB as a surfactant (Figure 8b) exhibited higher inhibition percentage compared to the CDC sample, CTAB-free synthesized, (Figure 8a). For instance, the highest inhibition percentage for CDC nanoparticle was found to be 21.10% for *Pseudomonas aeruginosa* and 19.69% for *Staphylococcus areas* at nanoparticles amount of 3 mg/mL, whereas was about 22.24% for *Klebsiella pneumoniae* at nanoparticles amount of 2 mg/mL. For CDC-CTAB nanoparticle, the maximum inhibition percentage was approximately 31.07% for *Pseudomonas aeruginosa* at nanoparticles amount of 2 mg/mL,

while 34.08% and 29.54% for *Klebsiella pneumoniae* and *Staphylococcus aureus* at nanoparticles amount of 3 mg/mL, respectively. The better inhibition percentage of CDC-CTAB nanoparticles is due to their smaller crystallite size (16.26 nm) and high surface area (56.72 m<sup>2</sup>/g) compared to CDC nanoparticles which have larger crystallite size (23.93 nm) and smaller surface area (24.54 m<sup>2</sup>/g). It was also reported in the literature that Gd-doped ceria nanoparticles (8% mol) with smaller crystallite size (57.40 nm) exhibited better antibacterial activity compared to other Gd-doped ceria nanoparticles (2 to 6 mol%) with bigger crystallite sizes (57.99-57.56 nm) [25].

According to Dickson and Koohmaraie [47], both types of bacteria (Gram-negative and Gram-positive) have a negatively charged surface. Thus, the antibacterial mechanism of the synthesized Ca-doped ceria nanoparticles might be due to

different steps. In the first, Ca-doped ceria nanoparticles (positively charged) will be adsorbed onto the bacterial membrane (negatively charged) through the electrostatic interaction. This leads to the penetration of small-sized ceria nanoparticles inside the bacterial cell wall and damaging the cell. In the second step, bacteria might be damaged through chemical degradation of the microorganism cells by the generated reactive oxygen species (ROS) [10, 23, 24].

Although the low inhibition percentage of both types of bacteria (Gram-negative and Gram-positive), the prepared nanomaterials can be considered as promising materials in terms of materials cost and toxicity compared to Ag nanoparticles. Besides, the inhibition percentage can be improved by altering the culture conditions such as medium pH and temperature [48, 49].

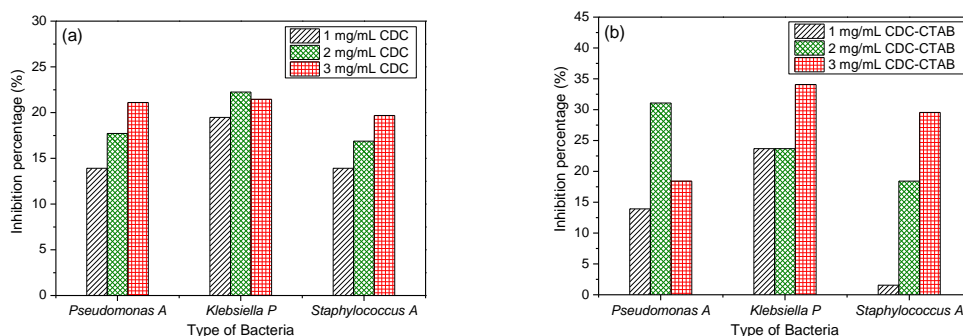


**Figure 8.** Inhibition percentage of various types of bacteria treated with amounts of nanomaterials. (a) CDC nanoparticles; (b) CDC-CTAB nanoparticles

## Conclusions

In this research study, the antibacterial potential of Ca-doped ceria nanoparticles against *Pseudomonas aeruginosa*, *Klebsiella pneumoniae* and *Staphylococcus aureus* (multi-drug resistant bacteria, MDR) was successfully evaluated using the optical density measurement method. Ca-doped ceria nanoparticles were synthesized via a co-precipitation method in the absence or the presence of a cationic surfactant (CTAB-assisted co-precipitation synthesis). The XRD results revealed that the CTAB-assisted synthesized Ca-doped ceria (CDC-CTAB) exhibited the lowest crystallite size (16.26 nm) and highest surface area (56.72 m<sup>2</sup>/g) compared to the CTAB-free synthesized Ca-doped ceria, CDC, (crystallite size of 23.93 nm and surface area of 24.54 m<sup>2</sup>/g). The antibacterial studies demonstrated that the bacterial growth depended on the amounts Ca-

doped ceria nanoparticles. In addition, the CDC-CTAB samples which have the highest surface area and smaller crystallite size exhibited the best inhibition percentages (29.54-34.08%) for all types of bacteria. The results revealed that the CDC-CTAB nanoparticles are promising materials, and their antibacterial activity might be evaluated against other types of antibiotic-resistant bacteria.

## Acknowledgement

The authors are thankful to the Department of Chemistry, Sebha University, Sebha, Libya for supporting this work. The authors would like to appreciate the Department of Botany (Microbiology Lab), Sebha University, Sebha, Libya for providing the isolated bacteria. The authors also thank **Dr. Hafad Alaswed** from Department of Statistics Department, Sebha

University for his assistance with SPSS analysis. The authors also would like to acknowledge the Criminal Investigation Department, Branch Sabha City for FTIR and UV instruments. The authors are grateful to **Eng. Asma Marei** and **Eng. Hussan Kut** from the Libyan Petroleum Institute, Tripoli, Libya for performing XRD analysis.

### Disclosure statement

No potential conflict of interest was reported by the authors.

### ORCID

Ibrahim A. Amar : 0000-0003-2354-0272

Shamsi A. Shamsi : 0000-0001-9941-5019

Mabroukah A. Abdulqadir : 0000-0003-1674-9211

Ihssin A. Abdalsamed : 0000-0002-5573-8374

### References

- [1] A. Gupta, S. Mumtaz, C.H. Li, I. Hussain, V.M. Rotello, *Chem. Soc. Rev.*, **2019**, 48, 415–427.
- [2] P.V. Baptista, M.P. McCusker, A. Carvalho, D.A. Ferreira, N.M. Mohan, M. Martins, A.R. Fernandes, *Front. Microbiol.*, **2018**, 9, 1441.
- [3] C.H. Wang, Y.H. Hsieh, Z.M. Powers, C.Y. Kao, *Int. J. Mol. Sci.*, **2020**, 21, 1061.
- [4] M.M. Hossain, S.A. Polash, M. Takikawa, R.D. Shubhra, T. Saha, Z. Islam, S. Hossain, M.A. Hasan, S. Takeoka, S.R. Sarker, *Front. Bioeng. Biotech.*, **2019**, 7, 239.
- [5] K.M. Ahmad, A.A. Alamen, F.A. Atiya, A.A. Elzen, *J. Adv. Lab. Res. Biol.*, **2018**, 9, 1–8.
- [6] K.M. Ahmad, A.A. Alamen, *JOPAS.*, **2019**, 18, 11–16.
- [7] K.M. Ahmad, A.A.M. Alamen, S.A.M.S. Shamsi, A.A. Elzen, *Med. J. Islamic World Acad. Sci.*, **2019**, 27, 9–16.
- [8] I.A.C.G. United, No Time to Wait: Securing the future from drug-resistant infections, in: *Report to the Secretary-General of the United Nations*, **2019**.
- [9] M. Qi, W. Li, X. Zheng, X. Li, Y. Sun, Y. Wang, C. Li, L. Wang, *Front. Mater.*, **2020**, 7, 213.
- [10] M. Zhang, C. Zhang, X. Zhai, F. Luo, Y. Du, C. Yan, *Sci. China. Mater.*, **2019**, 62, 1727–1739.
- [11] W. Abdussalam-Mohammed, *Adv. J. Chem. A*, **2020**, 3, 192–210.
- [12] S. Stankic, S. Suman, F. Haque, J. Vidic, *J. Nanobiotechnol.*, **2016**, 14, 1–20.
- [13] P.V. AshaRani, G. Low Kah Mun, M.P. Hande, S. Valiyaveetil, *ACS Nano*, **2009**, 3, 279–290.
- [14] A.P. Ingle, N. Duran, M. Rai, *Appl. Microbiol. Biotechnol.*, **2014**, 98, 1001–1009.
- [15] N. Thakur, P. Manna, J. Das, *J. Nanobiotechnol.*, **2019**, 17, 84.
- [16] F. Huang, J. Wang, W. Chen, Y. Wan, X. Wang, N. Cai, J. Liu, F. Yu, *J. Taiwan Inst. Chem. Eng.*, **2018**, 83, 40–49.
- [17] D.S. Tsai, T.S. Yang, Y.S. Huang, P.W. Peng, K.L. Ou, *Int. J. Nanomedicine*, **2016**, 11, 2531.
- [18] P.D. Tam, C.X. Thang, *Mater. Sci. Eng. C*, **2016**, 58, 953–959.
- [19] B.C. Nelson, M.E. Johnson, M.L. Walker, K.R. Riley, C.M. Sims, *Antioxidants*, **2016**, 5, 15.
- [20] S. Parvathya, B. Venkatramanb, *J. Nanosci. Curr. Res.*, **2017**, 2, 1–9.
- [21] S. Patil, S. Reshetnikov, M.K. Haldar, S. Seal, S. Mallik, *J. Phys. Chem. C*, **2007**, 111, 8437–8442.
- [22] K. Govindarasu, K. Gnanasekaran, S. Balaraman, B. Iruson, S. Krishnamoorthy, B. Padmaraj, E. Manikandan, S. Dhananjayan, *J. Nanosci. Lett.*, **2019**, 9, 1–16.
- [23] A. Balamurugan, M. Sudha, S. Surendhiran, R. Anandarasu, S. Ravikumar, Y.S. Khadar, *Mater. Today: Proceedings*, **2020**, 26, 3588–3594.
- [24] Y.S. Khadar, A. Balamurugan, V. Devarajan, R. Subramanian, S.D. Kumar, *J. Mater. Res. Technol.*, **2019**, 8, 267–274.
- [25] Y.S. Khadar, A. Balamurugan, V. Devarajan, R. Subramanian, *Orient. J. Chem.*, **2017**, 33, 2405–2411.

- [26] S. Banerjee, P.S. Devi, D. Topwal, S. Mandal, K. Menon, *Adv. Funct. Mater.*, **2007**, 17, 2847–2854.
- [27] I.A. Amar, M.M. Ahwidi, M. Zidan, I. Abdalsamed, A. Ali, *LJST*, **2018**, 7, 127–132.
- [28] K. Zhao, Y. Du, *J. Power Sources*, **2017**, 347, 79–85.
- [29] I.A. Amar, H.M. Harara, Q.A. Baqul, M.A. Abdulqadir, F.A. Altohami, M.M. Ahwidi, I.A. Abdalsamed, F.A. Saleh, *Asian J. Nanosci. Mater.*, **2020**, 3, 1–14.
- [30] L. Truffault, M.T. Ta, T. Devers, K. Konstantinov, V. Harel, C. Simmonard, C. Andreazza, I.P. Nevirkovets, A. Pineau, O. Veron, J.P. Blondeau, *Mater. Res. Bull.*, **2010**, 45, 527–535.
- [31] M. Nyoka, Y.E. Choonara, P. Kumar, P.P. Kondiah, V. Pillay, *Nanomaterials.*, **2020**, 10, 242.
- [32] J.T. Shang, M. Yang, W.L. Zhang, C. Tan, D.J. Han, *Appl. Mech. Mater.*, **2013**, 268, 180–183.
- [33] B. Jain, A.K. Singh, A. Hashmi, M.A.B.H. Susan, J.P. Lellouche, *Adv. Compos. Hybrid Mater.*, **2020**, 3, 430–441.
- [34] H. Li, G. Wang, F. Zhang, Y. Cai, Y. Wang, I. Djerdj, *Rsc Adv*, **2012**, 2, 12413–12423.
- [35] Z. Mosayebi, M. Rezaei, N. Hadian, F.Z. Kordshuli, F. Meshkani, *Mater. Res. Bull.*, **2012**, 47, 2154–2160.
- [36] Q. Zhang, J. Yang, Y.N. Gao, C.Y. Li, L. Sun, *Appl Petrochem. Res.*, **2015**, 5, 247–253.
- [37] A.P. Amaliya, S. Anand, S. Pauline, *J. Nanosci. Tech.*, **2016**, 186–188.
- [38] Y. Ma, X. Wang, H.A. Khalifa, B. Zhu, M. Muhammed, *Int. J. Hydrogen Energy*, **2012**, 37, 19401–19406.
- [39] H.Y. He, J. Lu, *Sep. Purif. Technol.*, **2017**, 172, 374–381.
- [40] B. Elahi, M. Mirzaee, M. Darroudi, R.K. Oskuee, K. Sadri, M.S. Amiri, *Ceram. Int.*, **2019**, 45, 4790–4797.
- [41] A.A. Athawale, M.S. Bapat, P.A. Desai, *J. Alloys Compd.*, **2009**, 484, 211–217.
- [42] R. Murugana, L. Kashinath, R. Subash, P. Sakthivel, K. Byrappa, S. Rajendran, G. Ravi, *Mater. Res. Bull.*, **2018**, 97, 319–235.
- [43] D.M.D.M. Prabakaran, K. Sadaiyandi, M. Mahendran, S. Sagadevan, *Mater. Res.*, **2016**, 19, 478–482.
- [44] S. Gnanam, V. Rajendran, *J. Alloys. Compd.*, **2018**, 735, 1854–1862.
- [45] R.P. Senthilkumar, V. Bhuvaneshwari, R. Ranjithkumar, S. Sathiyavimal, V. Malayaman, B. Chandarshekar, *Int. J. Biol. Macromol.*, **2017**, 104, 1746–1752.
- [46] D.H. Kim, J.C. Park, G.E. Jeon, C.S. Kim, J.H. Seo, *Biotechnol. Bioprocess Eng.*, **2017**, 22, 210–217.
- [47] J.S. Dickson, M. Koohmaraie, *Appl. Environ. Microbiol.*, **1989**, 55, 832–836.
- [48] E. Alpaslan, B.M. Geilich, H. Yazici, T.J. Webster, *Sci Rep*, **2017**, 7, 1–12.
- [49] M. Saliyani, R. Jalal, E.K. Goharshadi, *Jundishapur. J. Microbiol.*, **2015**, 8, e17115
- [40] P. Aberoomand Azar, F. Farjami, M. Saber Tehrani, E. Eslami, *Int. J. Electrochem. Sci.*, **2014**, 9, 2535–2547.

#### HOW TO CITE THIS ARTICLE

Ibrahim A. Amar\*, Shamsi A. Shamsi, Ruqayah M. Saheem, Amdallah A. Altawati, Mohammed A. Abdulkarim, Mabroukah A. Abdulqadir, Ihssin A. Abdalsamed. Surfactant-Assisted Co-Precipitation Synthesis of Ca-Doped Ceria Nanoparticles for Antibacterial Applications. *Adv. J. Chem. A*, 2021, 4(1), 10-21.

DOI: 10.22034/AJCA.2020.247227.1210

URL: [http://www.ajchem-a.com/article\\_117941.html](http://www.ajchem-a.com/article_117941.html)